


**First-principles study of the spin-orbit coupling contribution to anisotropic magnetic interactions**Di Wang,<sup>1,2</sup> Xiangyan Bo,<sup>3</sup> Feng Tang,<sup>1,2</sup> and Xiangang Wan<sup>1,2,4,\*</sup><sup>1</sup>National Laboratory of Solid State Microstructures and School of Physics, Nanjing University, Nanjing 210093, China<sup>2</sup>Collaborative Innovation Center of Advanced Microstructures, Nanjing University, Nanjing 210093, China<sup>3</sup>Nanjing University of Posts and Telecommunications, Nanjing 210023, China<sup>4</sup>Hefei National Laboratory, Hefei 230088, China (Received 29 December 2022; revised 10 May 2023; accepted 16 August 2023; published 28 August 2023)

Anisotropic magnetic exchange interactions lead to a surprisingly rich variety of magnetic properties. Considering the spin-orbit coupling (SOC) as perturbation, we extract the general expression of a bilinear spin Hamiltonian, including isotropic exchange interaction, antisymmetric Dzyaloshinskii-Moriya (DM) interaction, and symmetric  $\Gamma$  term. We derive the expressions for the second-order SOC contribution to DM interaction, and reveal that the essential distinction between the DM and  $\Gamma$  term is from their different hopping processes, rather than the different orders of SOC. Based on combining the magnetic force theorem and linear-response approach, we present a method of calculating anisotropic magnetic interactions, which now has been implemented in the open source software WIENJ. Furthermore, we introduce another method which could calculate the first- and second-order SOC contribution to the DM interaction separately, and overcome some shortcomings of previous methods. Our methods are successfully applied to several typical weak ferromagnets for  $3d$ ,  $4d$ , and  $5d$  transition-metal oxides. We also predict the conditions where the DM interactions proportional to  $\lambda$  approximately vanish while the DM interactions proportional to  $\lambda^2$  are nonzero, and believe that it may exist in certain magnetic materials.

DOI: [10.1103/PhysRevB.108.085140](https://doi.org/10.1103/PhysRevB.108.085140)**I. INTRODUCTION**

Magnetic properties can be typically described by a quadratic spin Hamiltonian, which is the basis of most magnetic theoretical investigations [1–4]. Generally, spin-orbit coupling (SOC) always exists and leads to the anisotropic magnetic interactions with low symmetry. The general form of the bilinear expression of a spin-exchange Hamiltonian could be written as

$$H = \sum_{i<j} J_{ij} \mathbf{S}_i \cdot \mathbf{S}_j + \sum_{i<j} \mathbf{D}_{ij} \cdot [\mathbf{S}_i \times \mathbf{S}_j] + \sum_{i<j} \mathbf{S}_i \cdot \Gamma_{ij} \cdot \mathbf{S}_j, \quad (1)$$

where the first term describes the isotropic Heisenberg Hamiltonian, the second one represents the Dzyaloshinskii-Moriya (DM) [5–7] interaction, and the third one is marked as the  $\Gamma$  term [6]. The antisymmetric DM interaction, which comes from the combination of low symmetry and SOC, was introduced by Dzyaloshinskii [5] and Moriya [6] in a phenomenological model and a microscopic model, respectively. Generally, DM interaction favors twisted spin structures and is constrained by the crystal symmetry. For example, when an inversion center is located at the bond center of two magnetic ion sites, the DM interaction between these two magnetic ions should be zero due to its antisymmetric property [6,8]. Now the DM interaction is invoked to explain numerous interesting magnetic systems featuring noncollinear spin textures, such

as weak ferromagnets [5,6], helimagnets [9], skyrmion formation [10–12], and chiral domain walls [13,14]. In addition, the DM interaction also plays an important role in multiferroic materials [15–19], topological magnon materials [20–22], and spintronics [23]. It is worth mentioning that, since DM interactions are very sensitive to small atomic displacements and symmetry restrictions, it can also be used to reveal the interplay of delicate structural distortions and complex magnetic configurations [24].

Recently, the first-principles study of magnetic exchange interactions, especially DM interaction, has also attracted much interest [3,25–52]. A popular numerical method is the energy-mapping analysis [3,25,26] to estimate magnetic interactions from the energy differences of various magnetic structures. However, this approach becomes inconvenient for the complicated systems where it is not clear how many exchange interactions needs to be considered, since in some magnetic compounds the magnetic moments may couple over a variety of distances, and even the ninth-nearest-neighbor coupling plays an important role [28,29]. Meanwhile, in itinerant magnetic systems, the magnetism is not so localized and the calculated magnetic moments may depend on the magnetic configurations, which also significantly affects the accuracy of the calculated DM interactions. Another approach using total energy differences could extract DM strength by directly calculating the energies of spirals with the finite vector  $q$  [30–35]. Meanwhile, an efficient approach is proposed based on the magnetic force theorem [27,36–48]. Katsnelson and Lichtenstein [37] derived the expression for DM interaction term based on Green's function approach. This method is applied to a large number of magnetic materials

\*Corresponding author: [xgwan@nju.edu.cn](mailto:xgwan@nju.edu.cn)

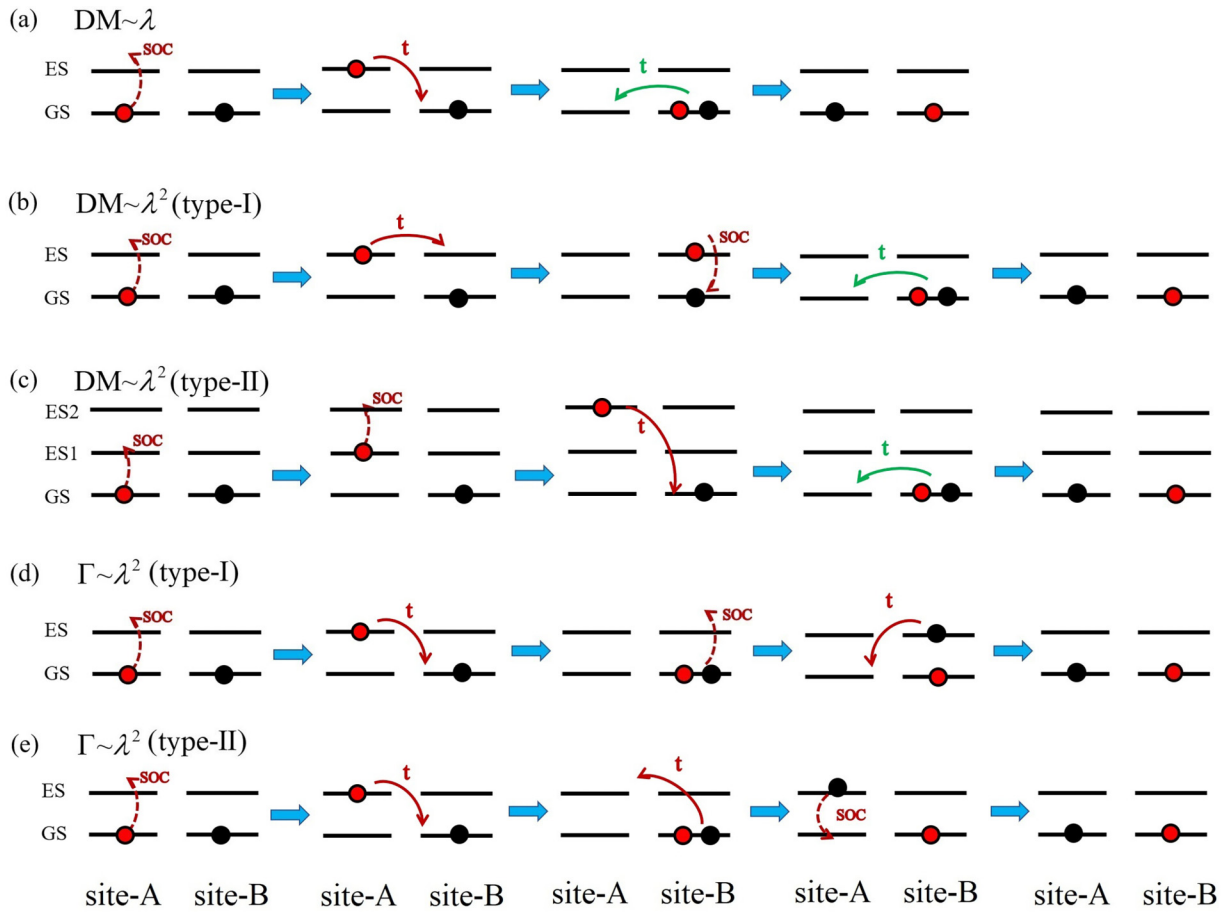


FIG. 1. Schematic pictures of exchange paths for anisotropic magnetic interactions between site A and site B. The dotted line represents the SOC excitation process, while the solid line represents the hopping process. (a) represents the DM interactions for the first order of SOC. The DM interactions for the second order of SOC have two types of perturbation processes, (b) and (c). Meanwhile, the perturbation processes for the symmetric  $\Gamma$  term are also shown in (d) and (e) for comparison. Here GS and ES represent ground state and excited state, respectively. It is worth mentioning that the perturbation processes of DM interactions involve the hopping between GSs, denoted by the green solid line. Meanwhile,  $\Gamma$  terms would only involve the hopping processes between GS and ES.

such as the antiferromagnets with weak ferromagnetism [38], thin magnetic films [41], diluted magnetic semiconductors [42], and various other magnetic materials [39,44–47]. This Green’s function approach was previously formulated in first-principles codes with direct definition of a localized orbitals basis set such as the linear muffin-tin orbitals method [53]. Furthermore, they also developed the method of calculating DM interactions using Wannier function formalism [40,43]. In addition, DM interactions could also be estimated by computing the long-wavelength limit of the spin susceptibility [49], the expectation value of the spin current density [50,51], or utilizing Berry phase [52].

In Ref. [6], Moriya considered the transfer integral  $C$  terms up to the first order of the SOC, and concluded that the terms linear in the SOC have the antisymmetric form for the interchange of two spins, while the terms of second order in the SOC have the pseudodipolar form which is symmetric for the two spins [6,7]. However, this often leads to overlooking the exist of second-order SOC correction to DM interactions. As shown in Refs. [4,54,55], many researchers believe that the magnitude of DM interaction is proportional to the SOC strength. Meanwhile, in the first-principles study

of DM interactions, there are many approaches with only the first-order SOC contribution to DM interactions being considered [38,39]. On the other hand, in these approaches using total energy differences, such as energy-mapping [3,25,26], spirals approach [31,32], and the approaches through calculating energy variations due to spin rotations [37,56,57], one can get the entire DM interaction but cannot distinguish the contribution from which order of SOC.

In this paper, we use perturbation theory to obtain expressions for the DM interaction up to the second-order terms of SOC, and find that the second-order SOC contribution to the antisymmetric DM interaction and symmetric  $\Gamma$  interaction arise from different hopping processes as shown in Fig. 1 and following. We extend the method of calculating Heisenberg interactions based on combining magnetic force theorem and linear-response approach [27,28,56–59] to estimate DM and  $\Gamma$  interactions, and the algorithm of our proposed method is now implemented in the open source called WIENJ [60] as an interface to the linearized augmented plane wave software WIEN2K [61]. Furthermore, to overcome some shortcomings of previous methods, we develop a method that can estimate the first- and second-order SOC contribution to the DM exchange

couplings separately. While our methods can also calculate  $\Gamma$  interaction, here we only present the results of Heisenberg and DM interactions since they could be compared with many previous works. We have applied our methods to several representatives of canted antiferromagnetic materials  $\text{La}_2\text{CuO}_4$ ,  $\text{Ca}_2\text{RuO}_4$ , and  $\text{Ca}_3\text{LiOsO}_6$  for  $3d$ ,  $4d$ , and  $5d$  transition-metal oxides, and the calculation results are consistent with the experiment. Particularly, we find that the DM interaction proportional to  $\lambda^2$  cannot be ignored in  $4d$  transition-metal oxide  $\text{Ca}_2\text{RuO}_4$ , and the DM interactions proportional to  $\lambda$  and  $\lambda^2$  have the same magnitude in  $5d$  transition-metal oxide  $\text{Ca}_3\text{LiOsO}_6$ . As shown in the following, the DM interactions proportional to  $\lambda$  and  $\lambda^2$  involve different exchange channels. Thus, based on the symmetry analysis, we explore the possibility that the DM interactions proportional to  $\lambda$  approximately vanish while the DM interactions proportional to  $\lambda^2$  still exist. We believe that this case could exist in certain magnetic materials.

## II. METHOD

### A. Anisotropic magnetic interactions by perturbation theory

We start from an effective model,

$$\begin{aligned} H &= H_0 + H_t + H_U + H_{\text{SOC}} \\ &= \sum_{i\alpha\sigma} \varepsilon_\alpha c_{i\alpha\sigma}^+ c_{i\alpha\sigma} + \sum_{ij\alpha\beta\sigma} t_{\alpha\beta}^{ij} c_{i\alpha\sigma}^+ c_{j\beta\sigma} \\ &\quad + \frac{U}{2} \sum_i n_i(n_i - 1) + \sum_i \lambda \mathbf{l}_i \cdot \mathbf{s}_i, \end{aligned} \quad (2)$$

where  $H_0$ ,  $H_t$ ,  $H_U$ , and  $H_{\text{SOC}}$  represent the on-site orbital energy, the hopping term, the Hubbard  $U$  term, and the SOC term, respectively. Here  $i, j$  represent the site index, while  $\alpha, \beta$  represent the orbital index and  $\sigma$  represents the spin index.  $n_i$  represents the number of electron operators at site  $i$ . We consider the on-site Coulomb interactions between two interacting electrons and neglect the dependence of the orbital indices, since the difference between intraorbital coupling  $U$  and interorbital coupling  $U'$  is usually smaller than the on-site Coulomb interaction. Meanwhile, only the on-site SOC effect  $\sum_i \lambda \mathbf{l}_i \cdot \mathbf{s}_i$  [4] is taken into account, and Eq. (2.6) of Ref. [6], which is related to Rashba-type SOC that can be sizable at surfaces and in layered materials, are not included here. We consider the spin-exchange interaction between the magnetic ions located at site  $A$  and site  $B$ . We label the ground state and the unoccupied states at site  $A$  as  $n$  and  $m$ , respectively. Similarly, the ground state and the excited states at site  $B$  are labeled as  $n'$  and  $m'$ , respectively.

When SOC is not considered, the Heisenberg interactions  $H_{\text{eff}} = J \mathbf{S}_A \cdot \mathbf{S}_B$  can be obtained by considering the hopping term as perturbations for the case of  $U \gg t$  [62]. Considering the SOC term  $\lambda \mathbf{l} \cdot \mathbf{s}$  as perturbation, the first-order SOC contribution to effective spin model  $H_{\text{eff}}^{(1)}$  has the expression of antisymmetric DM interaction as  $H_{\text{eff}}^{(1)} = \mathbf{D}^{(1)}(\mathbf{S}_A \times \mathbf{S}_B)$ , where  $\mathbf{D}^{(1)}$  could be written as [6]

$$(\mathbf{D}^\alpha)^{(1)} = -4i \frac{\lambda t_{nn'}}{U} \left( \sum_m \frac{l_{mn}^\alpha}{\varepsilon_m - \varepsilon_n} t_{mn'} - \sum_{m'} \frac{l_{m'n'}^\alpha}{\varepsilon_{m'} - \varepsilon_{n'}} t_{m'n} \right). \quad (3)$$

Meanwhile, by considering perturbation theory up to the second-order SOC correction (see details in the Appendix), we find that the second-order SOC correction has a contribution to both the DM term  $\mathbf{D}^{(2)}$  and the  $\Gamma$  term, where  $\mathbf{D}^{(2)}$  could be written as

$$\begin{aligned} (\mathbf{D}^\alpha)^{(2)} &= 2 \frac{\lambda^2 t_{nn'}}{U} \sum_{m, m'} \frac{l_{m'n'}^\beta l_{mn}^\gamma - l_{m'n'}^\gamma l_{mn}^\beta}{(\varepsilon_{m'} - \varepsilon_{n'}) (\varepsilon_m - \varepsilon_n)} t_{mm'} \\ &\quad - 2 \frac{\lambda^2 t_{nn'}}{U} \sum_{m_1, m_2} \frac{l_{m_1 m_2}^\beta l_{m_2 n}^\gamma - l_{m_1 m_2}^\gamma l_{m_2 n}^\beta}{(\varepsilon_{m_1} - \varepsilon_n) (\varepsilon_{m_2} - \varepsilon_n)} t_{m_1 n'} \\ &\quad + 2 \frac{\lambda^2 t_{nn'}}{U} \sum_{m'_1, m'_2} \frac{l_{m'_1 m'_2}^\beta l_{m'_2 n'}^\gamma - l_{m'_1 m'_2}^\gamma l_{m'_2 n'}^\beta}{(\varepsilon_{m'_1} - \varepsilon_{n'}) (\varepsilon_{m'_2} - \varepsilon_{n'})} t_{m'_1 n}. \end{aligned} \quad (4)$$

Meanwhile, the expression of parameter  $\Gamma^{(2)}$  could be seen in Eq. (A7) of the Appendix. Here the SOC contributions are given up to the second order. The high-order contributions are usually relatively smaller, since they would involve the excited states with higher energy.

Here we present schematic pictures of the exchange processes in Fig. 1. It is easy to see that the bilinear spin exchange Hamiltonian should contain two hopping processes between two sites A and B as shown in Fig. 1. The biquadratic spin exchange interaction comes from the fourth order of hopping term, which is not included here. Considering up to the second-order perturbation of SOC, we find that there are several different exchange processes. Among them, the first-order SOC correction has only a DM contribution  $\mathbf{D}^{(1)}$ , as shown in Fig. 1(a), which represents the first term of Eq. (3). When swapping sites A and B in Fig. 1(a), one can obtain the second term of Eq. (3). Meanwhile, the second-order SOC correction not only has the contribution to DM interaction but also the contribution to the  $\Gamma$  term as shown in Figs. 1(b)–1(e). While type-I  $\mathbf{D}^{(2)}$  as shown in Fig. 1(b) represents the first term of Eq. (4), type-II  $\mathbf{D}^{(2)}$  as shown in Fig. 1(c) represents the second term of Eq. (4), and the third term of Eq. (4) could be obtained by swapping sites A and B. It is worth mentioning that the exchange processes for DM interactions [Figs. 1(a)–1(c)] involve the hopping between ground states, which is denoted by the green solid line in Fig. 1 and  $t_{nn'}$  in Eqs. (3) and (4), respectively. In sharp contrast, there are only hoppings between ground states and excited states in the processes of  $\Gamma$  terms as shown in Figs. 1(d)–1(e). In Ref. [6], Moriya considered the transfer integral  $C$  up to the first order of the SOC and concluded that the antisymmetric DM interaction is linear with respect to the SOC while the second-order SOC contribution is the symmetric  $\Gamma$  term. If  $C$  terms had been given up to the high order of SOC, the DM terms from high-order SOC may also exist. Here we emphasize that, as shown in Fig. 1, the essential difference between the DM and  $\Gamma$  term is from their different hopping processes rather than the different orders of SOC.

### B. Magnetic interactions in the first-principles approach

First, we present the method to calculate magnetic interactions based on the force theorem and linear-response approach

[27,56,57], which could be written as the following form [56]:

$$J_{\mathbf{R}_l+\boldsymbol{\tau},\mathbf{R}_{l'+\boldsymbol{\tau}'}}^{\alpha\beta} = \sum_{nkn'k'} \frac{f_{nk} - f_{n'k'}}{\varepsilon_{nk} - \varepsilon_{n'k'}} \langle \psi_{nk} | [\boldsymbol{\sigma} \times \mathbf{B}_{\boldsymbol{\tau}}]_{\alpha} | \psi_{n'k'} \rangle \times \langle \psi_{n'k'} | [\boldsymbol{\sigma} \times \mathbf{B}_{\boldsymbol{\tau}'}]_{\beta} | \psi_{nk} \rangle e^{i(k'-k)(\mathbf{R}_l - \mathbf{R}_{l'})}. \quad (5)$$

This method has been successfully applied to calculate Heisenberg interactions in various magnetic materials [27,28,56–59]. This method allows one to calculate interactions in momentum space [63], thus one can easily calculate long-range exchange interactions even in complicated three-dimensional spin-web compounds like  $\text{Cu}_3\text{TeO}_6$  [28]. Considering the case of  $\alpha \neq \beta$ , we extend this method to estimate DM and  $\Gamma$  interactions, and the algorithm of this method is now implemented in the open source called WIENJ [60], as an interface to WIEN2K [61]. It is worth mentioning that the general expression of bilinear spin exchange parameter  $J^{\alpha\beta}$ , which could be written in  $J$ ,  $D$  and  $\Gamma$  as Eq. (1), has nine independent components. However, one can only yield four out of nine components of  $J^{\alpha\beta}$  for a given magnetic configuration. For example, for the collinear magnetic configuration with all spin moments lying along the  $z$  axis, only the four spin exchange parameters  $J^{xx}$ ,  $J^{yy}$ ,  $J^{xy}$ , and  $J^{yx}$  can be estimated. Therefore, to obtain the full nine spin-exchange parameters  $J^{\alpha\beta}$  (i.e.,  $J$ ,  $D$ , and  $\Gamma$  terms), one need perform different first-principles self-consistent calculations for at least three independent orientations of the magnetization [28]. Based on the self-consistent results from different spin orientations, the magnetic interactions could be calculated from Eq. (5) [28]. However, these self-consistent calculations by choosing three different spin orientations would produce 12 parameters, resulting in that sets of parameters  $J^{\alpha\beta}$  are not necessarily unique, naturally leading to the calculation deviation.

To reduce this calculation deviation, we also propose a method when SOC is relatively small. First, we perform the standard LSDA (+ $U$ ) calculations. Based on the eigenvalues  $\varepsilon_{nk}$  and eigenstates  $\psi_{nk}^{(0)}$  from LSDA (+ $U$ ) calculations, we take SOC as a perturbation and estimate the first-order and second-order SOC corrections, wave functions  $\psi_{nk}^{(1)}$  and  $\psi_{nk}^{(2)}$  in WIEN2K [61]. Then all  $J^{\alpha\beta}$  elements can be calculated without doing the separate self-consistent calculations with different spin orientations. Meanwhile, this method can produce the first- and second-order SOC contributions to the DM interaction separately.

The difference between the calculations using WIENJ and the second approach is that the wave functions in WIENJ are calculated self-consistently for a given spin configuration, whereas the second approach includes SOC corrections to the wave function via perturbation theory. Comparing the results of these two methods in the following, it can be seen that the calculated DM interaction in WIENJ has a similar value as the sum of the first- and second-order SOC contribution to the DM interaction, which implies that the higher-order SOC contributions are relatively small.

In the following, we will apply our two methods to several typical examples corresponding to  $3d$ ,  $4d$ , and  $5d$  transition metal oxides, respectively, in the next section.

TABLE I. The calculated Heisenberg exchange parameters  $J$  (in meV) for  $\text{La}_2\text{CuO}_4$ . The calculated spin-exchange parameters in the previous theoretical work are also shown for comparison.

$J$	$\text{La}_2\text{CuO}_4$		
	Ref. [57]	Ref. [38]	This paper
$J_1$	27.2	29.2	25.76
$J_2$	−3.00	−4.1, −3.9	−3.80, −3.38
$J_3$	−0.05	0	−0.11

### III. RESULTS

#### A. First-principles examples of typical materials

##### 1. $\text{La}_2\text{CuO}_4$

As a benchmark on the accuracy of our methods in calculating Heisenberg and DM interactions, we first study the famous  $\text{La}_2\text{CuO}_4$ , which have been studied in a number of theoretical works [38,40,57,64–68]. The LSDA+ $U$ (=7 eV) [69] calculation is applied. Without SOC considered, the calculated Heisenberg exchange parameters have no difference between these two approaches, which are summarized in Table I. The calculated nearest-neighbor magnetic coupling  $J_1$  are dominant with a value of about 25.76 meV. We can find that the spin-exchange coupling parameters decrease rapidly with the increasing distance between two Cu ions. The next-nearest-neighbor magnetic coupling  $J_2$  shows ferromagnetic behavior and is one order of magnitude smaller than  $J_1$ . The third-nearest-neighbor  $J_3$  is antiferromagnetic and almost negligible. The results agree well with previous theoretical work [38,57].

The weak ferromagnetism of  $\text{La}_2\text{CuO}_4$  is originated from the canting of the magnetic moments, which can be described by the competition of Heisenberg interaction and DM interaction. Based on the two approaches in above section, the nearest-neighbor DM parameters are calculated as shown in Table II. As shown in Table II, the DM interactions proportional to  $\lambda^2$  are negligible due to the small SOC in the  $3d$  orbital, and the DM interactions proportional to  $\lambda$  using the second approach are almost the same as the calculated DM parameters in WIENJ. According to the calculated Heisenberg and DM parameters, the value of the canting angle is estimated to be about  $1.7 \times 10^{-3}$ , which is in a good agreement with the experimental value of  $2.2\text{--}2.9 \times 10^{-3}$  [67,68]. For comparison with previous theoretical works, Mazurenko and Anisimov [38] proposed the angle value of  $0.7 \times 10^{-3}$  using Green's function technique. With the construction of a tight-binding parametrization of the Hamiltonian with SOC, Katsnelson *et al.* [40] calculated the canting angle to be  $5.0 \times 10^{-3}$ . It can be seen that our results agree well with the experimental and theoretical ones.

##### 2. $\text{Ca}_2\text{RuO}_4$

As the example of  $4d$  transition-metal oxides,  $\text{Ca}_2\text{RuO}_4$  crystallizes in the space group  $Pbca$  and has the layered perovskite structure [70–75]. The ground state of  $\text{Ca}_2\text{RuO}_4$  is an antiferromagnetic spin ordering with an insulating electrical behavior [71]. A weak ferromagnetic component is induced

TABLE II. The calculated nearest-neighbor DM interaction parameters (in meV) for  $\text{La}_2\text{CuO}_4$  via the two approaches in this paper.  $R$  is the radius vector from two sites of magnetic ions in units of the lattice constant. The columns  $D^{(1)}$  and  $D^{(2)}$  represent the calculated DM interaction proportional to  $\lambda$  and  $\lambda^2$ . Due to the small SOC, the DM interactions proportional to  $\lambda^2$  are zero, with an accuracy of 0.01 meV.

$R$	WIENJ	The second method in this paper	
	$D$	$D^{(1)}$	$D^{(2)}$
(0.5, -0.5, 0)	(-0.09, -0.14, 0)	(-0.09, -0.14, 0)	(0, 0, 0)
(-0.5, -0.5, 0)	(-0.09, 0.14, 0)	(-0.09, 0.14, 0)	(0, 0, 0)
(-0.5, 0.5, 0)	(-0.09, -0.14, 0)	(-0.09, -0.14, 0)	(0, 0, 0)
(0.5, 0.5, 0)	(-0.09, 0.14, 0)	(-0.09, 0.14, 0)	(0, 0, 0)

by spin canting below the magnetic transition temperature 113 K [70].

To study its magnetic properties, we performed the LSDA+ $U$  ( $=3eV$ ) [72] calculations for  $\text{Ca}_2\text{RuO}_4$ . The calculated nearest-neighbor Heisenberg interaction is about 20.9 meV. Experimentally, the Heisenberg parameters were estimated via inelastic neutron scattering as 16 meV in Ref. [74] and 5.8 meV in Ref. [75], and our result 20.9 meV is closer to the first value. Meanwhile, the calculated DM interactions by the two approaches mentioned above are both presented in Table III. As shown in Table III, the calculated DM interactions in WIENJ are also almost the same as the sum of DM interactions proportional to  $\lambda$  and  $\lambda^2$ , i.e.,  $D \approx D(\lambda) + D(\lambda^2)$ . This implies that the higher-order SOC contributions are relatively small. Note that the strength of first-order SOC corrected DM interactions  $|D(\lambda)|$  is around 1.31–1.41 meV, while the  $|D(\lambda^2)|$  is about 0.44 meV, therefore the DM interactions proportional to  $\lambda^2$  are non-negligible in such 4d magnetic system. The ratio of DM interactions and Heisenberg interaction is estimated to be  $|D|/J \approx 0.05$ , which is in good agreement with the rough estimate 0.06 from experiment [73].

### 3. $\text{Ca}_3\text{LiOsO}_6$

In 5d transition-metal oxide systems, the strength of SOC is expected to be stronger than 3d or 4d materials due to the large atomic number. However, in orbital singlet states with a relatively large electronic gap such as  $5d^3$  with half-filling  $t_{2g}$  orbitals [76], the electronic structures from fully self-consistent LSDA (+ $U$ ) + SOC calculation and the ones from further one iteration of SOC calculation after LSDA (+ $U$ ) calculation have a small difference (see Fig. 2 in the Appendix), indicating that the effect of SOC is still small [76].

As one concrete  $5d^3$  example, we focus on  $\text{Ca}_3\text{LiOsO}_6$  [76–79] with the crystal structure of  $\text{K}_4\text{CdCl}_6$  type. The

ground state of  $\text{Ca}_3\text{LiOsO}_6$  is antiferromagnetic (AFM) with the magnetic transition temperature 117 K. Both the first-principles study and the experiment suggest that  $\text{Ca}_3\text{LiOsO}_6$  has a fully opened electronic gap [78]. Though the AFM ordered state has been confirmed experimentally, the magnetization curve suggests a soft magnetism with a small spontaneous magnetization. The net magnetization is about  $0.02 \mu_B$  per  $\text{Os}^{5+}$  ion and is suggested due to a DM interaction generated by the broken inversion symmetry [76].

We perform the LSDA+ $U$  calculations of  $\text{Ca}_3\text{LiOsO}_6$  with  $U = 2 \text{ eV}$  [80–83] and calculate the magnetic interactions by applying our methods. The Heisenberg interactions  $J_1$ ,  $J_2$ , and  $J_3$  are estimated to be all AFM with the values of 13.1 meV, 5.5 meV, and 1.1 meV, respectively.  $J_1$  is the strongest spin exchange, while  $J_2$  is slightly less than one-half of  $J_1$ , and  $J_3$  is an order of magnitude smaller than  $J_1$ . These properties are consistent with the energy-mapping results, though our calculated spin parameters are slightly larger than theirs (9.9 meV, 4.1 meV, and 0.63 meV for  $J_1$ – $J_3$ , respectively) [79]. Meanwhile, our numerical DM interactions by the two approaches mentioned in the Method section are both summarized in Table IV. Since the DM interactions between the 3rd nearest neighbor and longer-range distances for  $\text{Os}^{5+}$  ions are negligible, thus we only show the DM interactions for the nearest neighbor and next-nearest neighbor in Table IV. It can be seen that the DM interactions proportional to  $\lambda^2$  have the same order of magnitude as the one proportional to  $\lambda$  in  $\text{Ca}_3\text{LiOsO}_6$ . According to the crystal symmetry, the nearest-neighbor  $D_1$  has the form of  $(0, 0, D_2)$ , and the calculated  $D_1$  via the two approaches are summarized in Table IV. Meanwhile, there are three different directions of  $D_2$  connected by the symmetry of threefold rotation along the  $z$  axis, as shown in last three rows of Table IV. Summarizing the DM parameters of all nearest neighbors and the isotropic spin-exchange parameters  $J$  up to the third-nearest neighbor, the expected net magnetic moment

TABLE III. The calculated DM interaction parameters (in meV) for  $\text{Ca}_2\text{RuO}_4$  via the two approaches in this paper. Here  $R$  is the radius vector from two sites of magnetic ions in units of the lattice constant. The columns  $D^{(1)}$  and  $D^{(2)}$  represent the calculated DM interaction proportional to  $\lambda$  and  $\lambda^2$ . It can be seen that the calculated interactions via these two approaches are close, i.e.,  $D \approx D^{(1)} + D^{(2)}$ .

$R$	WIENJ	The second method in this paper	
	$D$	$D^{(1)}$	$D^{(2)}$
(0.5, -0.5, 0)	(0.50, -1.03, 0.17)	(0.47, -1.19, 0.60)	(0.04, 0.15, -0.41)
(-0.5, 0.5, 0)	(0.50, -1.03, 0.17)	(0.47, -1.19, 0.60)	(0.04, 0.15, -0.41)
(-0.5, -0.5, 0)	(-0.43, -0.95, 0.17)	(-0.40, -1.10, 0.59)	(-0.04, 0.15, -0.41)
(0.5, 0.5, 0)	(-0.43, -0.95, 0.17)	(-0.40, -1.10, 0.59)	(-0.04, 0.15, -0.41)

TABLE IV. The calculated DM interaction parameters (in meV) for  $\text{Ca}_3\text{LiOsO}_6$  via the two approaches in this paper.  $R$  is the radius vector from two sites of magnetic ions in units of the lattice constant. The columns  $D^{(1)}$  and  $D^{(2)}$  represent the calculated DM interaction proportional to  $\lambda$  and  $\lambda^2$ .

$R$	WIENJ	The second method in this paper	
	$D$	$D^{(1)}$	$D^{(2)}$
(0.5, 0.5, 0.5)	(0, 0, -0.263)	(0, 0, -0.223)	(0, 0, -0.099)
(-0.5, 0.5, 0.5)	(-0.125, 0.205, -0.021)	(-0.083, 0.143, -0.052)	(-0.055, 0.095, 0.005)
(0.5, -0.5, 0.5)	(-0.125, -0.205, -0.021)	(-0.083, -0.143, -0.052)	(-0.055, -0.095, 0.005)
(0.5, 0.5, -0.5)	(0.226, 0, -0.021)	(0.165, 0, -0.052)	(0.110, 0, 0.005)

is estimated to be  $0.03 \mu_B$ , which is in good agreement with the experimental value of  $0.02 \mu_B$  [76].

### B. Materials with the second-order SOC contribution to DM interactions

Here we discuss the necessary conditions where the first order of SOC in DM interactions (i.e.,  $\mathbf{D}^{(1)}$ ) are approximately absent, while DM interactions proportional to the second order of SOC (i.e.,  $\mathbf{D}^{(2)}$ ) are dominant. According to the picture of Fig. 1 and Eqs. (3) and (4), when the excited states with higher energy could be ignored, we only consider the orbital ground state and the lowest-energy excited states at each site, and summarize these three conditions that need to be met:

(1) The hopping processes between the ground state and excited state ( $t_{mm'}$  and  $t_{m'n}$ ) are symmetry forbidden.

(2) The hopping between ground states ( $t_{mm'}$ ) and the hopping between excited states at two sites ( $t_{mm'n}$ ) are nonzero.

(3) The relation of orbital angular momentum of the two magnetic ions  $l_{m'n}^\beta l_{mn}^\gamma - l_{m'n'}^\gamma l_{mn}^\beta$  should be also nonzero.

According to the first condition  $t_{mm'} = t_{m'n} = 0$ , the exchange processes in Figs. 1(a) and 1(c) are forbidden, therefore  $\mathbf{D}^{(1)}$  is constrained to zero. Meanwhile, the second and third conditions make the exchange processes in Fig. 1(b) exist, thus  $\mathbf{D}^{(2)}$  could be present. Based on these restrictions, one can predict possible candidates with only the second-order SOC contribution to DM interactions according to their different combinations of crystal symmetry, Wyckoff sites and orbital occupation pattern. In the Appendix, we present a concrete magnetic model where the first order of SOC in DM interactions vanish approximately. However, in real materials, the high-energy excited states always exist and the  $\mathbf{D}^{(1)}$  could be small but not strictly zero. We believe that  $\mathbf{D}^{(2)}$  could be dominant in certain magnetic materials, which deserves further research.

## IV. CONCLUSION

The magnetic model plays an important role in magnetic investigations. Here we revisit the general expression of magnetic interactions, including isotropic exchange interaction, antisymmetric DM interaction and symmetric  $\Gamma$  term. We clarify that the DM and  $\Gamma$  interactions can be separated from their different hopping processes rather than the orders of SOC. We present two first-principles methods to calculate the anisotropic magnetic interactions. Based on the first method, one need perform self-consistent calculations for at least three different spin orientations to obtain the full nine exchange parameters  $J^{\alpha\beta}$ . On the other hand, using the second method, one can estimate these magnetic exchange parameters with no need to do the separate self-consistent calculations for different spin orientations. This method can also calculate the first-order and second-order SOC contributions to DM interactions separately. We have successfully applied our methods to several typical weak ferromagnetic materials  $\text{La}_2\text{CuO}_4$ ,  $\text{Ca}_2\text{RuO}_4$ , and  $\text{Ca}_3\text{LiOsO}_6$ , respectively. Furthermore, according to the microscopic mechanism shown in Fig. 1, we list three necessary conditions which can lead to the DM interactions proportional to  $\lambda$  approximately vanishing while the DM interactions proportional to  $\lambda^2$  exist.

## ACKNOWLEDGMENTS

This work was supported by the NSFC (No. 12188101, 11834006, 12004170), National Key R&D Program of China (No. 2022YFA1403601), Natural Science Foundation of Jiangsu Province, China (Grant No. BK20200326), the excellent program in Nanjing University, and Innovation Program for Quantum Science and Technology (No. 2021ZD0301902). X.W. also acknowledges the support from the Tencent Foundation through the XPLOER PRIZE.

## APPENDIX

### 1. The anisotropic magnetic interactions proportional to $\lambda$ and $\lambda^2$

Based on the effective model written as Eq. (2) in the main text, the magnetic interactions can be obtained by considering the hopping term and the SOC term as perturbations. Without SOC, the effective spin model is the isotropic Heisenberg model [62]. We further take into account the impact of SOC. As mentioned in the main text, we label the ground state and the unoccupied states without SOC considered at site  $A$  as  $|\psi_n^{(0)}\rangle$  and  $|\psi_m^{(0)}\rangle$ , respectively. Taking  $\lambda I_A \cdot s_A$  as a perturbation, we can obtain the first-order and second-order SOC corrected wave functions  $|\psi_n^{(1)}\rangle$  and  $|\psi_n^{(2)}\rangle$ . Meanwhile, the wave functions at site  $B$  have the similar expressions by simply replacing  $n, m$  by  $n', m'$ . Based on the perturbation theory, the first-order SOC contribution could

be written as

$$\begin{aligned} & - \sum_{R \in \mathcal{L}'} \frac{\langle \phi_I^{(1)} | H_I | \phi_R^{(0)} \rangle \langle \phi_R^{(0)} | H_I | \phi_J^{(0)} \rangle}{U} - \sum_{R \in \mathcal{L}'} \frac{\langle \phi_I^{(0)} | H_I | \phi_R^{(1)} \rangle \langle \phi_R^{(0)} | H_I | \phi_J^{(0)} \rangle}{U} \\ & - \sum_{R \in \mathcal{L}'} \frac{\langle \phi_I^{(0)} | H_I | \phi_R^{(0)} \rangle \langle \phi_R^{(1)} | H_I | \phi_J^{(0)} \rangle}{U} - \sum_{R \in \mathcal{L}'} \frac{\langle \phi_I^{(0)} | H_I | \phi_R^{(0)} \rangle \langle \phi_R^{(0)} | H_I | \phi_J^{(1)} \rangle}{U}, \end{aligned} \quad (\text{A1})$$

where  $\phi_I$  and  $\phi_J$  belong to the model space of ground states  $\mathcal{L}$ , while  $\phi_R$  belongs to the space of excited states  $\mathcal{L}'$ . The superscript ( $n$ ) represents the  $n$ th order of SOC perturbation. After substituting the SOC corrected wave functions into the above equation, it is easy to find that the first-order SOC contribution of the effective spin model  $H_{\text{eff}}^{(1)}$  has the expression of DM interaction as

$$H_{\text{eff}}^{(1)} = \mathbf{D}^{(1)}(\mathbf{S}_A \times \mathbf{S}_B), \quad (\text{A2})$$

where  $\mathbf{D}^{(1)}$  could be written as [i.e., Eq. (3) in the main text] [6]

$$(D^\alpha)^{(1)} = -4i \frac{\lambda t_{nn'}}{U} \left( \sum_m \frac{l_{mn}^\alpha}{\varepsilon_m - \varepsilon_n} t_{mm'} - \sum_{m'} \frac{l_{m'n'}^\alpha}{\varepsilon_{m'} - \varepsilon_{n'}} t_{m'n} \right). \quad (\text{A3})$$

The second-order SOC contribution could be written as

$$\begin{aligned} & - \sum_{R \in \mathcal{L}'} \frac{\langle \phi_I^{(1)} | H_I | \phi_R^{(0)} \rangle \langle \phi_R^{(1)} | H_I | \phi_J^{(0)} \rangle}{U} - \sum_{R \in \mathcal{L}'} \frac{\langle \phi_I^{(0)} | H_I | \phi_R^{(1)} \rangle \langle \phi_R^{(0)} | H_I | \phi_J^{(1)} \rangle}{U} \\ & - \sum_{R \in \mathcal{L}'} \frac{\langle \phi_I^{(1)} | H_I | \phi_R^{(0)} \rangle \langle \phi_R^{(0)} | H_I | \phi_J^{(1)} \rangle}{U} - \sum_{R \in \mathcal{L}'} \frac{\langle \phi_I^{(0)} | H_I | \phi_R^{(1)} \rangle \langle \phi_R^{(1)} | H_I | \phi_J^{(0)} \rangle}{U} \\ & - \sum_{R \in \mathcal{L}'} \frac{\langle \phi_I^{(1)} | H_I | \phi_R^{(1)} \rangle \langle \phi_R^{(0)} | H_I | \phi_J^{(0)} \rangle}{U} - \sum_{R \in \mathcal{L}'} \frac{\langle \phi_I^{(0)} | H_I | \phi_R^{(0)} \rangle \langle \phi_R^{(1)} | H_I | \phi_J^{(1)} \rangle}{U} \\ & - \sum_{R \in \mathcal{L}'} \frac{\langle \phi_I^{(2)} | H_I | \phi_R^{(0)} \rangle \langle \phi_R^{(0)} | H_I | \phi_J^{(0)} \rangle}{U} - \sum_{R \in \mathcal{L}'} \frac{\langle \phi_I^{(0)} | H_I | \phi_R^{(2)} \rangle \langle \phi_R^{(0)} | H_I | \phi_J^{(0)} \rangle}{U} \\ & - \sum_{R \in \mathcal{L}'} \frac{\langle \phi_I^{(0)} | H_I | \phi_R^{(0)} \rangle \langle \phi_R^{(2)} | H_I | \phi_J^{(0)} \rangle}{U} - \sum_{R \in \mathcal{L}'} \frac{\langle \phi_I^{(0)} | H_I | \phi_R^{(0)} \rangle \langle \phi_R^{(0)} | H_I | \phi_J^{(2)} \rangle}{U}. \end{aligned} \quad (\text{A4})$$

There are in total ten terms, in which the first six terms come from the first-order corrected wave functions, and the last four terms come from the second-order corrected wave functions. After substituting the SOC-corrected wave functions into Eq. (A4), we find that the first four terms have the expression as the anisotropic symmetric  $\Gamma$  interaction, while the last six terms have the expression as the antisymmetric DM interaction.

Finally, the second-order SOC correction of effective Hamiltonian  $H_{\text{eff}}^{(2)}$  could be written as

$$H_{\text{eff}}^{(2)} = \mathbf{D}^{(2)}(\mathbf{S}_A \times \mathbf{S}_B) + \mathbf{S}_A \cdot \Gamma^{(2)} \cdot \mathbf{S}_B, \quad (\text{A5})$$

where  $\mathbf{D}^{(2)}$  could be written as [i.e., Eq. (4) in the main text]

$$\begin{aligned} (D^\alpha)^{(2)} &= 2 \frac{\lambda^2 t_{nn'}}{U} \sum_{m, m'} \frac{l_{m'n'}^\beta l_{mn}^\gamma - l_{m'n'}^\gamma l_{mn}^\beta}{(\varepsilon_{m'} - \varepsilon_{n'}) (\varepsilon_m - \varepsilon_n)} t_{mm'} - 2 \frac{\lambda^2 t_{nn'}}{U} \sum_{m_1, m_2} \frac{l_{m_1 m_2}^\beta l_{m_2 n}^\gamma - l_{m_1 m_2}^\gamma l_{m_2 n}^\beta}{(\varepsilon_{m_1} - \varepsilon_n) (\varepsilon_{m_2} - \varepsilon_n)} t_{m_1 n'} \\ &+ 2 \frac{\lambda^2 t_{nn'}}{U} \sum_{m'_1, m'_2} \frac{l_{m'_1 m'_2}^\beta l_{m'_2 n'}^\gamma - l_{m'_1 m'_2}^\gamma l_{m'_2 n'}^\beta}{(\varepsilon_{m'_1} - \varepsilon_{n'}) (\varepsilon_{m'_2} - \varepsilon_{n'})} t_{m'_1 n}. \end{aligned} \quad (\text{A6})$$

Here  $\{\alpha, \beta, \gamma\}$  represents  $\{x, y, z\}$ ,  $\{y, z, x\}$ , or  $\{z, x, y\}$ . Meanwhile, the anisotropic symmetric parameter  $\Gamma^{(2)}$  could be written as

$$\begin{aligned} (\Gamma^{\beta\gamma})^{(2)} &= 2 \frac{\lambda^2}{U} \sum_{m, m'} \frac{l_{m'n'}^\beta l_{mn}^\gamma + l_{m'n'}^\gamma l_{mn}^\beta}{(\varepsilon_{m'} - \varepsilon_{n'}) (\varepsilon_m - \varepsilon_n)} t_{mn'} t_{m'n} - 2 \frac{\lambda^2}{U} \sum_{m_1, m_2} \frac{l_{m_1 n}^\beta l_{m_2 n}^\gamma}{(\varepsilon_{m_1} - \varepsilon_n) (\varepsilon_{m_2} - \varepsilon_n)} t_{m_1 n'} t_{m_2 n'} \\ &- 2 \frac{\lambda^2}{U} \sum_{m'_1, m'_2} \frac{l_{m'_1 n'}^\beta l_{m'_2 n'}^\gamma}{(\varepsilon_{m'_1} - \varepsilon_{n'}) (\varepsilon_{m'_2} - \varepsilon_{n'})} t_{m'_1 n'} t_{m'_2 n} \quad (\text{for } \beta \neq \gamma), \end{aligned}$$

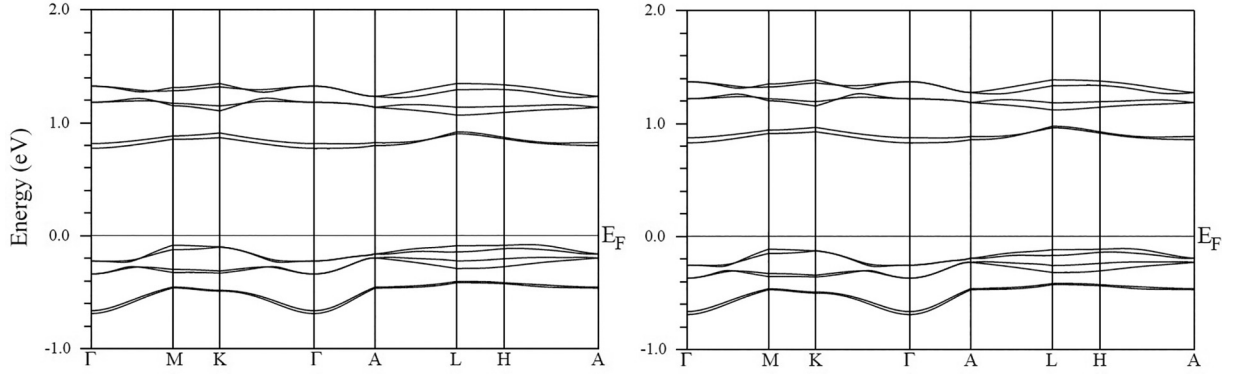


FIG. 2. (a) The electronic structures within fully self-consistent LSDA (+ $U$ )+SOC calculation of  $\text{Ca}_3\text{LiOsO}_6$ . (b) The electronic structures with one iteration of calculation with SOC after LSDA (+ $U$ ) calculation of  $\text{Ca}_3\text{LiOsO}_6$ . The value of  $U$  is set to be 2 eV.

$$\begin{aligned}
 (\Gamma^{\alpha\alpha})^{(2)} = & 4 \frac{\lambda^2}{U} \sum_{m,m'} \frac{l_{m'n'}^\alpha l_{mn}^\alpha}{(\varepsilon_{m'} - \varepsilon_{n'}) (\varepsilon_m - \varepsilon_n)} t_{mn'} t_{m'n} - 2 \frac{\lambda^2}{U} \sum_{m,m',\beta} \frac{l_{m'n'}^\beta l_{mn}^\beta}{(\varepsilon_{m'} - \varepsilon_{n'}) (\varepsilon_m - \varepsilon_n)} t_{mn'} t_{m'n} \\
 & - 2 \frac{\lambda^2}{U} \sum_{m_1,m_2} \frac{l_{m_1 n'}^\alpha l_{m_2 n}^\alpha}{(\varepsilon_{m_1} - \varepsilon_{n'}) (\varepsilon_{m_2} - \varepsilon_n)} t_{m_1 n'} t_{m_2 n} + \frac{\lambda^2}{U} \sum_{m_1,m_2,\beta} \frac{l_{m_1 n'}^\beta l_{m_2 n}^\beta}{(\varepsilon_{m_1} - \varepsilon_{n'}) (\varepsilon_{m_2} - \varepsilon_n)} t_{m_1 n'} t_{m_2 n} \\
 & - 2 \frac{\lambda^2}{U} \sum_{m'_1,m'_2} \frac{l_{m'_1 n'}^\alpha l_{m'_2 n}^\alpha}{(\varepsilon_{m'_1} - \varepsilon_{n'}) (\varepsilon_{m'_2} - \varepsilon_n)} t_{m'_1 n'} t_{m'_2 n} + \frac{\lambda^2}{U} \sum_{m'_1,m'_2,\beta} \frac{l_{m'_1 n'}^\beta l_{m'_2 n}^\beta}{(\varepsilon_{m'_1} - \varepsilon_{n'}) (\varepsilon_{m'_2} - \varepsilon_n)} t_{m'_1 n'} t_{m'_2 n}. \quad (\text{A7})
 \end{aligned}$$

## 2. The electronic structures of $\text{Ca}_3\text{LiOsO}_6$

Here we present the electronic structures of  $\text{Ca}_3\text{LiOsO}_6$ . In Fig. 2(a), the electronic structures from standard self-consistent LSDA (+ $U$ )+SOC calculation are shown. On the other hand, we perform the standard self-consistent LSDA (+ $U$ ) calculation. After this, we perform one more iteration of calculation with SOC considered. The corresponding electronic structures are shown in Fig. 2(b) for comparison. These band structures are almost the same, indicating the reliability of the second method for anisotropic magnetic interactions in this paper.

## 3. The magnetic model with the second-order SOC contribution to DM interactions

In the following, we present a concrete magnetic model where the first order of SOC in DM interactions (i.e.,  $\mathbf{D}^{(1)}$ )

vanish approximately, while DM interactions proportional to the second order of SOC (i.e.,  $\mathbf{D}^{(2)}$ ) are dominant. Here we focus on the well-known perovskite structures. In ideal perovskite structures, the nearest-neighbor DM coupling would vanish due to the inversion symmetry at the center of two  $M$  ions ( $M$  is the magnetic ion). Perovskite materials usually have lattice distortion, and we assume that the  $\text{MO}_6$  octahedra are rotated with respect to the  $z$  axis with staggered rotation angle  $\pm\theta$  as shown in Fig. 3(a). It leads to a doubling of the unit cell, and we denote the magnetic ions in these two sublattices as A and B both with  $(4/m)$  site symmetry, as shown in Fig. 3(b). The inversion symmetry at the center of A and B ions is broken, but the mirror symmetry within the  $xy$  plane is maintained while O ions are still located at the mirror plane, as shown in Fig. 3(b). Here we start from the effective model written as Eq. (2), and consider the term of on-site orbital energy first. Usually, the octahedral crystal field

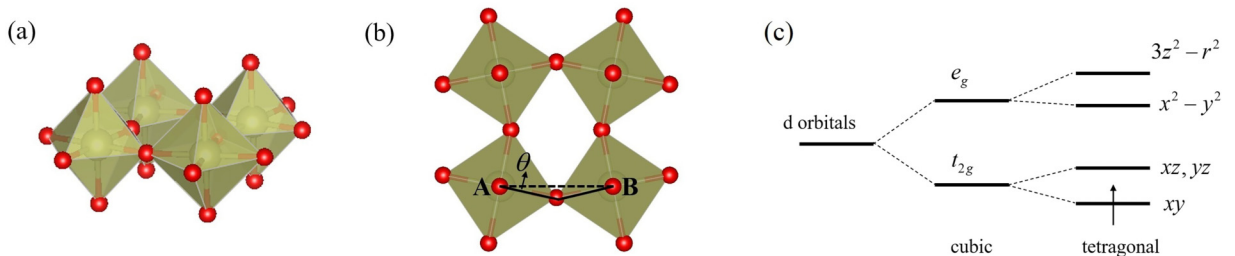


FIG. 3. (a) The distorted perovskite structures with the staggered rotation of neighboring oxygen octahedra by an angle  $\theta$  about the  $z$  axis. (b) A and B sublattices with a view of  $z$  direction. (c) The splitting and electron occupation pattern of  $d$  orbitals of  $M$  ions.



splitting between the  $e_g$  and  $t_{2g}$  levels is large, thus we can only consider the  $t_{2g}$  manifold. According to the tetragonal crystal field in each local coordinate, the  $t_{2g}$  orbitals would split into  $d_{xy}$  orbitals and twofold degenerate states  $d_{yz}/d_{zx}$ , as shown in Fig. 3(c). Here we assume the  $M$  magnetic ion to be  $d^1$  configuration. The ground orbital state of magnetic ion is  $d_{xy}$  orbital, and the on-site energy difference of these orbitals is labeled as  $\Delta = \varepsilon_{d_{yz}/d_{zx}} - \varepsilon_{d_{xy}}$ . Then we consider the hopping term between A and B magnetic ions lying in the same mirror plane. It is worth mentioning that the eigenvalues of the mirror operation for ground state  $d_{xy}$  and excited states  $d_{yz}/d_{zx}$  are +1 and -1, respectively. The hopping between the orbitals with different eigenvalues of mirror operation are symmetry forbidden, therefore the nearest-neighbor hopping matrix could be written as

$$H_t = \begin{bmatrix} t_0 & & \\ & t_1 & t_3 \\ & -t_3 & t_2 \end{bmatrix}, \quad (\text{A8})$$

where the left and right basis vectors are  $\{ \langle d_{xy}^A |, \langle d_{zx}^A |, \langle d_{yz}^A | \}$  and  $\{ |d_{xy}^B \rangle, |d_{zx}^B \rangle, |d_{yz}^B \rangle \}^T$ . Considering the mirror plane in-

cluding sites A and B, the DM interaction  $\mathbf{D}$  should be perpendicular to the mirror plane, which is along the  $z$  direction written as  $\mathbf{D} = (0, 0, D^z)$ . Using Eqs. (3) and (4), we can obtain the DM interaction proportional to  $\lambda$  or  $\lambda^2$ , which could be written as

$$(D^z)^{(1)} = 0, \\ (D^z)^{(2)} = 2 \frac{\lambda^2 t_0 [(t_1 + t_2) \sin 2\theta + 2t_3 \cos 2\theta]}{U \Delta^2}. \quad (\text{A9})$$

As shown above, the DM interactions proportional to  $\lambda$  are forbidden while the DM interactions proportional to  $\lambda^2$  are present. Notice that in the above magnetic model, the  $e_g$  orbitals are ignored since the crystal field splitting between the  $e_g$  and  $t_{2g}$  levels is usually large. When all the orbitals are considered, the DM interactions proportional to  $\lambda$  exist but should be relatively small. This anomalous DM interactions may exist in certain magnetic materials, and one can exploit our restraint conditions to predict promising candidates according to the combination of orbital occupation pattern and crystal symmetry.

- 
- [1] R. M. White, *Quantum Theory of Magnetism: Magnetic Properties of Materials* (Springer-Verlag, Berlin, Heidelberg, 2007).
- [2] K. H. J. Buschow and F. R. de Boer, *Physics of Magnetism and Magnetic Materials* (Springer, New York, 2003).
- [3] C. de Graaf and R. Broer, *Magnetic Interactions in Molecules and Solids* (Springer, New York, 2016).
- [4] D. I. Khomskii, *Transition Metal Compounds* (Cambridge University Press, Cambridge, England, 2014).
- [5] I. Dzyaloshinskii, A thermodynamic theory of “weak” ferromagnetism of antiferromagnetics, *J. Phys. Chem. Solids* **4**, 241 (1958).
- [6] T. Moriya, Anisotropic superexchange interaction and weak ferromagnetism, *Phys. Rev.* **120**, 91 (1960).
- [7] T. Moriya, New Mechanism of Anisotropic Superexchange Interaction, *Phys. Rev. Lett.* **4**, 228 (1960).
- [8] V. V. Mazurenko, Y. O. Kvashnin, A. I. Lichtenstein, and M. I. Katsnelson, A DMI guide to magnets micro-world, *J. Exp. Theor. Phys.* **132**, 506 (2021).
- [9] J. Kishine and A. S. Ovchinnikov, Theory of monoaxial chiral helimagnet, in *Solid State Physics* (Academic Press, New York, 2015), pp. 1–130.
- [10] U. K. Rössler, A. Bogdanov, and C. Pfleiderer, Spontaneous skyrmion ground states in magnetic metals, *Nature* **442**, 797 (2006).
- [11] N. Nagaosa and Y. Tokura, Topological properties and dynamics of magnetic skyrmions, *Nat. Nanotechnol.* **8**, 899 (2013).
- [12] A. Fert, N. Reyren, and V. Cros, Magnetic skyrmions: advances in physics and potential applications, *Nat. Rev. Mater.* **2**, 17031 (2017).
- [13] K.-S. Ryu, L. Thomas, S.-H. Yang, and S. Parkin, Chiral spin torque at magnetic domain walls, *Nat. Nanotechnol.* **8**, 527 (2013).
- [14] G. Chen, J. Zhu, A. Quesada, J. Li, A. T. N’Diaye, Y. Huo, T. P. Ma, Y. Chen, H. Y. Kwon, C. Won, Z. Q. Qiu, A. K. Schmid, and Y. Z. Wu, Novel Chiral Magnetic Domain Wall Structure in Fe/Ni/Cu (001) Films, *Phys. Rev. Lett.* **110**, 177204 (2013).
- [15] H. Katsura, N. Nagaosa, and A. V. Balatsky, Spin Current and Magnetoelectric Effect in Noncollinear Magnets, *Phys. Rev. Lett.* **95**, 057205 (2005).
- [16] I. A. Sergienko and E. Dagotto, Role of the Dzyaloshinskii-Moriya interaction in multiferroic perovskites, *Phys. Rev. B* **73**, 094434 (2006).
- [17] M. Mostovoy, Ferroelectricity in Spiral Magnets, *Phys. Rev. Lett.* **96**, 067601 (2006).
- [18] S.-W. Cheong and M. Mostovoy, Multiferroics: A magnetic twist for ferroelectricity, *Nat. Mater.* **6**, 13 (2007).
- [19] K. Wang, J.-M. Liu, and Z. Ren, Multiferroicity: The coupling between magnetic and polarization orders, *Adv. Phys.* **58**, 321 (2009).
- [20] L. Zhang, J. Ren, J.-S. Wang, and B. Li, Topological magnon insulator in insulating ferromagnet, *Phys. Rev. B* **87**, 144101 (2013).
- [21] Y. Su, X. S. Wang, and X. R. Wang, Magnonic Weyl semimetal and chiral anomaly in pyrochlore ferromagnets, *Phys. Rev. B* **95**, 224403 (2017).
- [22] J. Fransson, A. M. Black-Schaffer, and A. V. Balatsky, Magnon dirac materials, *Phys. Rev. B* **94**, 075401 (2016).
- [23] X. S. Wang, H. W. Zhang, and X. R. Wang, Topological Magnonics: A Paradigm for Spin-Wave Manipulation and Device Design, *Phys. Rev. Appl.* **9**, 024029 (2018).
- [24] H. Zhou, S. Yan, D. Fan, D. Wang, and X. Wan, Magnetic interactions and possible structural distortion in kagome FeGe from first-principles study and symmetry analysis, *Phys. Rev. B* **108**, 035138 (2023).
- [25] H. Xiang, C. Lee, H.-J. Koo, X. Gong, and M.-H. Whangbo, Magnetic properties and energy-mapping analysis, *Dalton Trans.* **42**, 823 (2013).
- [26] J. H. Yang, Z. L. Li, X. Z. Lu, M.-H. Whangbo, S.-H. Wei, X. G. Gong, and H. J. Xiang, Strong Dzyaloshinskii-Moriya

- Interaction and Origin of Ferroelectricity in  $\text{Cu}_2\text{OSeO}_3$ , *Phys. Rev. Lett.* **109**, 107203 (2012).
- [27] A. I. Liechtenstein, M. Katsnelson, V. Antropov, and V. Gubanov, Local spin density functional approach to the theory of exchange interactions in ferromagnetic metals and alloys, *J. Magn. Magn. Mater.* **67**, 65 (1987).
- [28] D. Wang, X. Bo, F. Tang, and X. Wan, Calculated magnetic exchange interactions in the Dirac magnon material  $\text{Cu}_3\text{TeO}_6$ , *Phys. Rev. B* **99**, 035160 (2019).
- [29] D. Wang, J. Yu, F. Tang, Y. Li, and X. Wan, Determining the range of magnetic interactions from the relations between magnon eigenvalues at high-symmetry  $k$  points, *Chin. Phys. Lett.* **38**, 117101 (2021).
- [30] S. V. Halilov, H. Eschrig, A. Y. Perlov, and P. M. Oppeneer, Adiabatic spin dynamics from spin-density-functional theory: Application to Fe, Co, and Ni, *Phys. Rev. B* **58**, 293 (1998).
- [31] M. Heide, G. Bihlmayer, and S. Blügel, Describing Dzyaloshinskii–Moriya spirals from first principles, *Phys. B: Condens. Matter* **404**, 2678 (2009).
- [32] M. Heide, G. Bihlmayer, and S. Blügel, Dzyaloshinskii–Moriya interaction accounting for the orientation of magnetic domains in ultrathin films: Fe/W(110), *Phys. Rev. B* **78**, 140403(R) (2008).
- [33] P. Ferriani, K. von Bergmann, E. Y. Vedmedenko, S. Heinze, M. Bode, M. Heide, G. Bihlmayer, S. Blügel, and R. Wiesendanger, Atomic-Scale Spin Spiral with a Unique Rotational Sense: Mn Monolayer on W(001), *Phys. Rev. Lett.* **101**, 027201 (2008).
- [34] L. M. Sandratskii, Insight into the Dzyaloshinskii–Moriya interaction through first-principles study of chiral magnetic structures, *Phys. Rev. B* **96**, 024450 (2017).
- [35] H. Yang, A. Thiaville, S. Rohart, A. Fert, and M. Chshiev, Anatomy of Dzyaloshinskii–Moriya Interaction at Co/Pt Interfaces, *Phys. Rev. Lett.* **115**, 267210 (2015).
- [36] P. Bruno, Exchange Interaction Parameters and Adiabatic Spin-Wave Spectra of Ferromagnets: A “Renormalized Magnetic Force Theorem,” *Phys. Rev. Lett.* **90**, 087205 (2003).
- [37] M. I. Katsnelson and A. I. Liechtenstein, First-principles calculations of magnetic interactions in correlated systems, *Phys. Rev. B* **61**, 8906 (2000).
- [38] V. V. Mazurenko and V. I. Anisimov, Weak ferromagnetism in antiferromagnets:  $\alpha\text{-Fe}_2\text{O}_3$  and  $\text{La}_2\text{CuO}_4$ , *Phys. Rev. B* **71**, 184434 (2005).
- [39] V. V. Mazurenko, S. L. Skornyakov, V. I. Anisimov, and F. Mila, First-principles investigation of symmetric and antisymmetric exchange interactions of  $\text{SrCu}_2(\text{BO}_3)_2$ , *Phys. Rev. B* **78**, 195110 (2008).
- [40] M. I. Katsnelson, Y. O. Kvashnin, V. V. Mazurenko, and A. I. Liechtenstein, Correlated band theory of spin and orbital contributions to Dzyaloshinskii–Moriya interactions, *Phys. Rev. B* **82**, 100403(R) (2010).
- [41] L. Udvardi, L. Szunyogh, K. Palotás, and P. Weinberger, First-principles relativistic study of spin waves in thin magnetic films, *Phys. Rev. B* **68**, 104436 (2003).
- [42] H. Ebert and S. Mankovsky, Anisotropic exchange coupling in diluted magnetic semiconductors: Ab initio spin-density functional theory, *Phys. Rev. B* **79**, 045209 (2009).
- [43] V. Dmitrienko, E. Ovchinnikova, S. Collins, G. Nisbet, G. Beutier, Y. Kvashnin, V. Mazurenko, A. Liechtenstein, and M. Katsnelson, Measuring the Dzyaloshinskii–Moriya interaction in a weak ferromagnet, *Nat. Phys.* **10**, 202 (2014).
- [44] S. Mankovsky and H. Ebert, Accurate scheme to calculate the interatomic Dzyaloshinskii–Moriya interaction parameters, *Phys. Rev. B* **96**, 104416 (2017).
- [45] I. Solovyev, N. Hamada, and K. Terakura, Crucial Role of the Lattice Distortion in the Magnetism of  $\text{LaMnO}_3$ , *Phys. Rev. Lett.* **76**, 4825 (1996).
- [46] A. N. Rudenko, V. V. Mazurenko, V. I. Anisimov, and A. I. Liechtenstein, Weak ferromagnetism in Mn nanochains on the CuN surface, *Phys. Rev. B* **79**, 144418 (2009).
- [47] Y. O. Kvashnin, A. Bergman, A. I. Liechtenstein, and M. I. Katsnelson, Relativistic exchange interactions in  $\text{CrX}_3$  ( $X = \text{Cl}, \text{Br}, \text{I}$ ) monolayers, *Phys. Rev. B* **102**, 115162 (2020).
- [48] I. V. Solovyev, Self-consistent linear response for the spin-orbit interaction related properties, *Phys. Rev. B* **90**, 024417 (2014).
- [49] T. Koretsune, N. Nagaosa, and R. Arita, Control of Dzyaloshinskii–Moriya interaction in  $\text{Mn}_{1-x}\text{Fe}_x\text{Ge}$ : a first-principles study, *Sci. Rep.* **5**, 13302 (2015).
- [50] T. Kikuchi, T. Koretsune, R. Arita, and G. Tatara, Dzyaloshinskii–Moriya Interaction as a Consequence of a Doppler Shift due to Spin-Orbit-Induced Intrinsic Spin Current, *Phys. Rev. Lett.* **116**, 247201 (2016).
- [51] T. Koretsune, T. Kikuchi, and R. Arita, First-principles evaluation of the Dzyaloshinskii–Moriya interaction, *J. Phys. Soc. Jpn.* **87**, 041011 (2018).
- [52] F. Freimuth, S. Blügel, and Y. Mokrousov, Berry phase theory of Dzyaloshinskii–Moriya interaction and spin–orbit torques, *J. Phys.: Condens. Matter* **26**, 104202 (2014).
- [53] O. K. Andersen and O. Jepsen, Explicit, First-Principles Tight-Binding Theory, *Phys. Rev. Lett.* **53**, 2571 (1984).
- [54] D. Dai, H. Xiang, and M.-H. Whangbo, Effects of spin-orbit coupling on magnetic properties of discrete and extended magnetic systems, *J. Comput. Chem.* **29**, 2187 (2008).
- [55] M.-H. Whangbo, H.-J. Koo, and D. Dai, Spin exchange interactions and magnetic structures of extended magnetic solids with localized spins: Theoretical descriptions on formal, quantitative and qualitative levels, *J. Solid State Chem.* **176**, 417 (2003).
- [56] X. Wan, Q. Yin, and S. Y. Savrasov, Calculation of Magnetic Exchange Interactions in Mott–Hubbard Systems, *Phys. Rev. Lett.* **97**, 266403 (2006).
- [57] X. Wan, T. A. Maier, and S. Y. Savrasov, Calculated magnetic exchange interactions in high-temperature superconductors, *Phys. Rev. B* **79**, 155114 (2009).
- [58] X. Wan, J. Dong, and S. Y. Savrasov, Mechanism of magnetic exchange interactions in europium monochalcogenides, *Phys. Rev. B* **83**, 205201 (2011).
- [59] X. Wan, V. Ivanov, G. Resta, I. Leonov, and S. Y. Savrasov, Exchange interactions and sensitivity of the Ni two-hole spin state to Hund’s coupling in doped  $\text{NdNiO}_2$ , *Phys. Rev. B* **103**, 075123 (2021).
- [60] D. Wang, X. Bo, F. Tang, and X. Wan, WienJ, <https://github.com/diwang0214/WienJ>.
- [61] P. Blaha, K. Schwarz, G. Madsen, D. Kvasnicka, and J. Luitz, *WIEN2k, An Augmented Plane Wave+ Local Orbitals Program for Calculating Crystal Properties* (Karlheinz Schwarz, TU Wien, Austria, 2001).
- [62] P. W. Anderson, Antiferromagnetism. theory of superexchange interaction, *Phys. Rev.* **79**, 350 (1950).

- [63] R. Yambe and S. Hayami, Effective spin model in momentum space: Toward a systematic understanding of multiple- $Q$  instability by momentum-resolved anisotropic exchange interactions, *Phys. Rev. B* **106**, 174437 (2022).
- [64] D. Coffey, T. M. Rice, and F. C. Zhang, Dzyaloshinskii-Moriya interaction in the cuprates, *Phys. Rev. B* **44**, 10112 (1991).
- [65] L. Shekhtman, O. Entin-Wohlman, and A. Aharony, Moriya's Anisotropic Superexchange Interaction, Frustration, and Dzyaloshinsky's Weak Ferromagnetism, *Phys. Rev. Lett.* **69**, 836 (1992).
- [66] T. Yildirim, A. B. Harris, A. Aharony, and O. Entin-Wohlman, Anisotropic spin Hamiltonians due to spin-orbit and Coulomb exchange interactions, *Phys. Rev. B* **52**, 10239 (1995).
- [67] T. Thio, T. R. Thurston, N. W. Preyer, P. J. Picone, M. A. Kastner, H. P. Jenssen, D. R. Gabbe, C. Y. Chen, R. J. Birgeneau, and A. Aharony, Antisymmetric exchange and its influence on the magnetic structure and conductivity of  $\text{La}_2\text{CuO}_4$ , *Phys. Rev. B* **38**, 905 (1988).
- [68] M. A. Kastner, R. J. Birgeneau, T. R. Thurston, P. J. Picone, H. P. Jenssen, D. R. Gabbe, M. Sato, K. Fukuda, S. Shamoto, Y. Endoh, K. Yamada, and G. Shirane, Neutron-scattering study of the transition from antiferromagnetic to weak ferromagnetic order in  $\text{La}_2\text{CuO}_4$ , *Phys. Rev. B* **38**, 6636 (1988).
- [69] Pan Wei and Zheng Qing Qi, Electronic structure of  $\text{La}_2\text{CuO}_4$  and  $\text{YBa}_2\text{Cu}_3\text{O}_6$ : A local-spin-density approximation with on-site Coulomb- $U$  correlation calculations, *Phys. Rev. B* **49**, 12159 (1994).
- [70] M. Braden, G. André, S. Nakatsuji, and Y. Maeno, Crystal and magnetic structure of  $\text{Ca}_2\text{RuO}_4$ : Magnetoelastic coupling and the metal-insulator transition, *Phys. Rev. B* **58**, 847 (1998).
- [71] H. Fukazawa, S. Nakatsuji, and Y. Maeno, Intrinsic properties of the mott insulator  $\text{Ca}_2\text{RuO}_4 + \delta$  ( $\delta = 0$ ) studied with single crystals, *Phys. B: Condens. Matter* **281-282**, 613 (2000).
- [72] J. H. Jung, Z. Fang, J. P. He, Y. Kaneko, Y. Okimoto, and Y. Tokura, Change of Electronic Structure in  $\text{Ca}_2\text{RuO}_4$  Induced by Orbital Ordering, *Phys. Rev. Lett.* **91**, 056403 (2003).
- [73] S. Kunkemöller, E. Komleva, S. V. Streltsov, S. Hoffmann, D. I. Khomskii, P. Steffens, Y. Sidis, K. Schmalzl, and M. Braden, Magnon dispersion in  $\text{Ca}_2\text{Ru}_{1-x}\text{Ti}_x\text{O}_4$ : Impact of spin-orbit coupling and oxygen moments, *Phys. Rev. B* **95**, 214408 (2017).
- [74] S. Kunkemöller, D. Khomskii, P. Steffens, A. Piovano, A. A. Nugroho, and M. Braden, Highly Anisotropic Magnon Dispersion in  $\text{Ca}_2\text{RuO}_4$ : Evidence for Strong Spin Orbit Coupling, *Phys. Rev. Lett.* **115**, 247201 (2015).
- [75] A. Jain, M. Krautloher, J. Porras, G. Ryu, D. Chen, D. Abernathy, J. Park, A. Ivanov, J. Chaloupka, G. Khaliullin *et al.*, Higgs mode and its decay in a two-dimensional antiferromagnet, *Nat. Phys.* **13**, 633 (2017).
- [76] Y. Shi, Y. Guo, S. Yu, M. Arai, A. Sato, A. A. Belik, K. Yamaura, and E. Takayama-Muromachi, Crystal growth and structure and magnetic properties of the 5d oxide  $\text{Ca}_3\text{LiOsO}_6$ : extended superexchange magnetic interaction in oxide, *J. Am. Chem. Soc.* **132**, 8474 (2010).
- [77] S. Calder, M. D. Lumsden, V. O. Garlea, J.-W. Kim, Y. G. Shi, H. L. Feng, K. Yamaura, and A. D. Christianson, Magnetic structure determination of  $\text{Ca}_3\text{LiOsO}_6$  using neutron and x-ray scattering, *Phys. Rev. B* **86**, 054403 (2012).
- [78] S. Calder, D. J. Singh, V. O. Garlea, M. D. Lumsden, Y. G. Shi, K. Yamaura, and A. D. Christianson, Interplay of spin-orbit coupling and hybridization in  $\text{Ca}_3\text{LiOsO}_6$  and  $\text{Ca}_3\text{LiRuO}_6$ , *Phys. Rev. B* **96**, 184426 (2017).
- [79] E. Kan, F. Wu, C. Lee, J. Kang, and M.-H. Whangbo, On the high magnetic-ordering temperature of the 5d magnetic oxide  $\text{Ca}_3\text{LiOsO}_6$  crystallizing in a trigonal crystal structure: Density functional analysis, *Inorg. Chem.* **50**, 4182 (2011).
- [80] X. Wan, A. M. Turner, A. Vishwanath, and S. Y. Savrasov, Topological semimetal and fermi-arc surface states in the electronic structure of pyrochlore iridates, *Phys. Rev. B* **83**, 205101 (2011).
- [81] Y. Du, X. Wan, L. Sheng, J. Dong, and S. Y. Savrasov, Electronic structure and magnetic properties of  $\text{NaOsO}_3$ , *Phys. Rev. B* **85**, 174424 (2012).
- [82] X. Wan, A. Vishwanath, and S. Y. Savrasov, Computational Design of Axion Insulators Based on 5d Spinel Compounds, *Phys. Rev. Lett.* **108**, 146601 (2012).
- [83] R. Arita, J. Kuneš, A. V. Kozhevnikov, A. G. Eguiluz, and M. Imada, *Ab Initio* Studies on the Interplay Between Spin-Orbit Interaction and Coulomb Correlation in  $\text{Sr}_2\text{IrO}_4$  and  $\text{Ba}_2\text{IrO}_4$ , *Phys. Rev. Lett.* **108**, 086403 (2012).